NUCLEAR SCIENCE AND TECHNIQUES **25**, 050603 (2014)

The effect of Nb additive on Te-induced stress corrosion cracking in Ni alloy: a first-principles calculation*

LIU Wen-Guan (刘文冠),[1,2] HAN Han (韩晗),[1,2] REN Cui-Lan (任翠兰),[1,3]
YIN Hui-Qin (阴慧琴),[1,2] HUAI Ping (怀平),[1,2] ZOU Yang (邹杨),[1,2] and XU Hong-Jie (徐洪杰)[1,2,†]

[1]*Shanghai Institute of Applied Physics, Chinese Academy of Sciences, Shanghai 201800, China*
[2]*Key Laboratory of Nuclear Radiation and Nuclear Energy Technology, Chinese Academy of Sciences, Shanghai 201800, China*
[3]*Key Laboratory of Interfacial Physics and Technology, Chinese Academy of Sciences, Shanghai 201800, China*

(Received December 31, 2013; accepted in revised form March 25, 2014; published online September 25, 2014)

Nb can improve the resistance of Ni-based Hastelloy N alloy to Te-induced intergranular embrittlement. First-principles calculations are performed to research this mechanism by simulating the Ni(111) surface and the $\sum 5(012)$ grain boundary. The calculated adsorption energy suggests that Te atoms prefer diffusing along the grain boundary to forming the surface-reaction layer with Nb on surface of the Ni alloy. First-principles tensile tests show that the Nb segregation can enhance the cohesion of grain boundary. The strong Nb-Ni bonding can prevent the Te migration into the inside of the alloy. According to the Rice-Wang model, the strengthening/embrittling energies of Nb and Te are calculated, along with their mechanical and chemical components. The chemical bonds and electronic structures are analyzed to uncover the physical origin of the different effects of Te and Nb. Our work sheds lights on the effect of Nb additive on the Te-induced intergranular embrittlement in Hastelloy N alloy on the atomic and electronic level.

Keywords: Nb, Hastelloy N, Te, First-principles calculations, Stress corrosion cracking, Molten salt reactor

DOI: 10.13538/j.1001-8042/nst.25.050603

I. INTRODUCTION

Molten Salt Reactor (MSR) is the only liquid-fueled reactor in the six most promising Generation IV reactor concepts [1]. As the structural material developed specially for MSR, Hastelloy N, a Ni-based alloy, has excellent corrosion resistance against molten salt, and was used in Molten Salt Reactor Experiment (MSRE) of the Oak Ridge National Laboratory (ORNL, USA). However, MSRE revealed that the usefulness of Hastelloy N is limited by its susceptibility to stress corrosion cracking (SCC) induced by Te, which is a most dangerous problem of Hastelloy N [2, 3]. Te, a fission product in fuel salt, tends to diffuse along the surface grain boundaries (GBs) of Hastelloy N and causes intergranular cracking eventually, which is related closely with SCC.

To tackle this problem, a straightforward approach is to modify Hastelloy N by added alloying materials. MSRE found that adding Nb (1%∼2%) to Hastelloy N was beneficial in reducing intergranular Te cracking, but still, it embrittled [4, 5]. The mechanism of the Nb effect on the Te-induced SCC is unknown: Nb may form a stable and innocuous telluride compound, or Nb hypothetically forms surface-reaction layers with Te in preference to the Te diffusion into the alloy along the GBs, and so on [4, 5]. So, studies on this mechanism shall be helpful for developing more advanced Ni alloys, with adequate resistance to Te, for MSR.

First-principles calculation is suitable to mechanism investigations at atomic level. It was used successfully in studying effects of dopants or impurities in GB [6–9]. In this paper, we perform a first-principles calculation to clarify this mechanism by simulating a $\sum 5(012)$ Ni GB [7, 10] and the Ni(111) surface with the coexistence of Te and Nb. The results about the effects of Te on Ni GB are in accordance with our previous work [9].

II. COMPUTATIONAL DETAILS

Figure 1 is a schematic diagram of a $\sum 5(012)$ Ni GB unit cell. It contains two reversely oriented grains with 80 Ni atoms. The atom layer is distinguished by the distance between the layer and the GB plane. The GB0 layer represents the hollow sites. There are four equivalent atomic sites in each layer. The geometry optimization calculation of GB was performed including cell optimization. We adopted the GB model in Ref. [7], and performed further optimization (including cell optimization) to find a more accurate GB model.

The Ni(111) surface is modeled by a slab with a (4×4) surface periodic cell, which contains six layers of Ni atoms. The calculated lattice constant of bulk Ni used to build the Ni(111) surface is 3.52 Å, which is in good agreement with the experimental result. The bottom layer without Te or Nb is fixed to its optimal bulk position to mimic the bulk. The vacuum layer is about 12 Å thick. The Nb-Ni(111) surface, with a Nb atom substituted for a Ni atom in the topmost layer of

* Supported by Science and Technology Commission of Shanghai Municipality (No. 11JC1414900), Project supported by the National Basic Research Program of China (No. 2010CB934501),Thorium Molten Salts Reactor Fund (No. XDA02000000), the National Natural Science Foundation of China (No. 11005148), the Special Presidential Foundation of the Chinese Academy of Science, China (No. 29), and the National Natural Science Foundation of China (No. 51371188)
† Corresponding author, xuhongjie@sinap.ac.cn

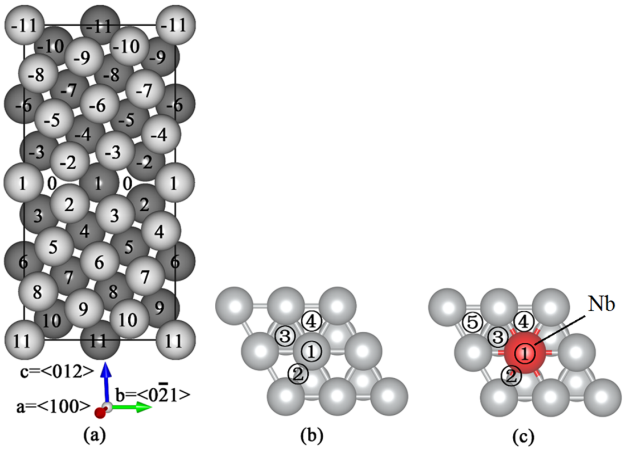

Fig. 1. (Color online) Schematic diagram of (a) unit cell of $\sum 5(012)$ Ni GB. The atomic sites are labeled by numbers counted from the GB plane. For clarity, the gray and black balls represent atoms in layers with $x = 0$ (in the paper plane) and $x = 0.25$ (beneath the paper plane) along the $\langle 100 \rangle$ direction, respectively. The other atoms with $x = 0.5$ and $x = 0.75$ are not shown. The right parts show the adsorption sites on the (111) surfaces of pure Ni (b) and Ni-Nb system (c): (1) (5) (1) top site; (2) bridge site; (3) hcp site; (4) fcc site.

the Ni(111) surface (Fig. 1(c)), are also calculated to compare with the Ni(111) surface.

Spin-polarized electronic state calculations were performed within the DFT [11, 12] using Vienna ab-initio simulation package (VASP) [13]. Projector-augmented plane-wave (PAW) [14] methods were employed with the PBE generalized gradient approximation (GGA) [15]. The wave functions were expanded in a plane-wave basis set with a cutoff energy of 350 eV. The Brillouin zone was sampled using a $3 \times 3 \times 1$ k-point mesh.

First-principles tensile tests were carried out to study the GB strength with Te or Nb in GB region. To simplify the calculations, the lattice dimensions in the GB plane were fixed to neglect the Poisson's ratio. A uniaxial tensile strain was exerted in the GB normal direction (i.e. the $\langle 012 \rangle$ direction). In each strain step, the starting atomic configuration is taken from the relaxed configuration of the preceding step by an increment of 2% to ensure the continuous strain path.

III. RESULTS AND DISCUSSION

A. Adsorption energy of Te

The adsorption energies of Te, E_{ad}, on the Ni(111) and Nb-Ni(111) surfaces are calculated by:

$$E_{\text{ad}} = E_{\text{Te-sub}} - E_{\text{atom,Te}} - E_{\text{sub}}, \quad (1)$$

where $E_{\text{Te-sub}}$, $E_{\text{atom,Te}}$ and E_{sub} refer to the calculated total energies of the optimized substrate with the adsorbate (i.e. a Te atom), one isolated Te atom, and the clean substrate, respectively. A strongly negative value of E_{ad} means intense binding between the Te atom and the substrate.

As shown in Fig. 1, the top, bridge, hexagonal close-packed (hcp), and face-centered cubic (fcc) sites were considered for the adsorption. Table 1 shows the calculated adsorption energies (in eV) of Te at each site on surface of Ni(111) and Nb-Ni(111), and the two data groups in three site types are roughly the same. These kinds of substitution of Nb for Ni do not change too much of the adsorption energy of Te, whereas the hcp site of Nb-Ni(111) is unstable for Te adsorption due to the existence of the Nb atom, and the Te atom is repelled to move from the hcp site to a farther site (Site 5 in Fig. 1(c)). As a result, Te atoms do not preferentially form the strong binding with Nb atoms on the surface of Ni-Nb alloy. So, the resistance of Nb to the Te-induced SCC in Hastelloy N cannot be attributed to the hypothetical formation of surface-reaction layers between Te and Nb. And Te would prefer to diffuse into the alloy along the GBs. The Nb effect in GB with the coexistence of Te will be discussed later.

TABLE 1. Adsorption energies (eV) of Te at different sites on the Ni(111) and Nb-Ni(111) surfaces (See Fig. 1 for the atomic sites)

Surface	top	bridge	hcp	fcc
Ni(111)	−3.37	−4.13	−4.18	−4.26
Ni(111)-Nb	−3.12	−4.05	unstable	−4.43

B. First-principles tensile tests

To further understand how the Nb additive affects the Ni GB at presence of Te, first-principles tensile tests were carried out to investigate the maximum strength of the GB and its fracture process. Te and Nb atoms, which are greater in size than Ni, prefer to occupy substitution sites (Site 1 in Fig. 1) rather than interstitial sites (Site 0 in Fig. 1) on the GB plane. So only the substitution case is considered. There are four sites in Layer 1. For simplification, the comparison was made among the clean GB, the GB + Nb layer (4 Nb atoms in Layer 1), the GB + mixed layer of Nb and Te (2 Nb and 2 Te in Layer 1), and the GB + Te layer.

As shown in Fig. 2, the GB + Nb layer has the largest tensile strength (21.3 GPa) at the strain of 28%, while that of the clean GB case is a little lower. On the other hand, the maximum strength of the GB + Te layer is about one-half of the case of GB + Nb layer. However, when the four sites in Layer 1 are occupied by 2 Nb and 2 Te atoms, the maximum GB strength increases to 16.4 GPa at the strain of 20%, which is obviously improved compared with the GB + Te layer. Clearly, Nb segregation enhances the Ni GB cohesion, and Te in the GB region induces the Ni GB embrittlement, hence the inhibition of the Te-induced SCC in Ni GB by the segregated Nb atoms.

In the region of strain $< 28\%$, the elastic deformation occurs for the GB + Nb layer. From strain = 32%∼36%, this GB undergoes the plastic deformation, and positions of the atoms in the GB cell are not layer by layer any longer. For the clean GB, GB + Te layer and GB + 2(Nb + Te), the frac-

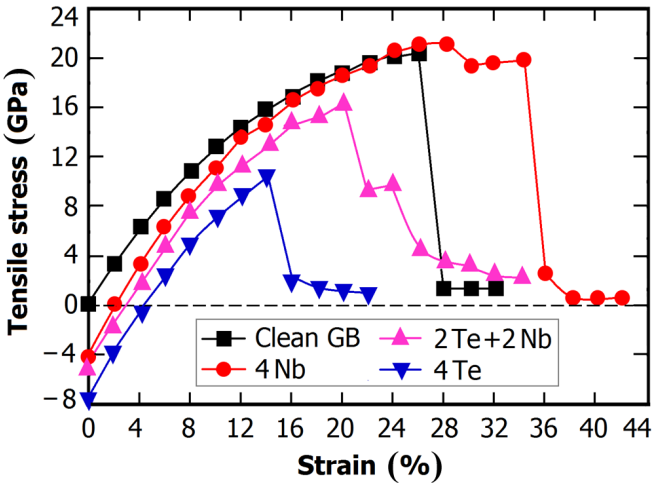

Fig. 2. (Color online) Calculated tensile stress as a function of strain for the clean GB, GB + Nb layer (4 Nb atoms in Layer 1), GB + mixed layer of Nb and Te (2 Nb and 2 Te atoms in Layer 1), and GB + Te layer.

ture surface of the GB is indeed the GB plane. However, the fracture surface of the GB + Nb layer is not the GB plane but the plane between the Layers 2 and 3 (See Fig. 1). As a result, the Nb(1)–Ni(2) bonds are stronger than the Ni(2)-Ni(3) bonds in the GB + Nb layer, and the corresponding Ni(1)-Ni(2) bonds in the clean GB.

C. Strengthening/embrittling energy

According to the Rice-Wang model [16], effects of the various elements on the GB cohesion can be determined by the strengthening/embrittling energy, ΔE, which is defined as

$$\Delta E = (E_{\mathrm{GB,doped}} - E_{\mathrm{GB}}) - (E_{\mathrm{FS,doped}} - E_{\mathrm{FS}}), \quad (2)$$

where, $E_{\mathrm{GB,doped}}$, E_{GB}, $E_{\mathrm{FS,doped}}$ and E_{FS} represent the total energies of the doped-GB, clean GB, doped-free surface (FS) and clean FS, respectively. A positive value of ΔE means embrittlement of the GB, and a negative value indicates enhancement of the GB.

To gain a deeper understanding, the strengthening/embrittling energy can be decomposed into the mechanical and chemical components. The procedure of decomposition in Refs. [10, 17–19] was used to perform the analysis.

The calculated ΔE and its mechanical and chemical components for Te and Nb are listed in Table 2. According to the calculated strengthening/embrittling energy, Te, with a positive value, is an embrittler, and Nb, with a negative value, is a cohesion enhancer. The mechanical components of Te and Nb are both positive. This is due to that the bigger atomic sizes of Te and Nb cause the GB expansion. On the other hand, the chemical component of Nb is strongly negative and plays a dominant role in the strengthening/embrittling energy. However, Te has a small value of the chemical component, which has little effect on the strengthening/embrittling energy. So, the contrary effects of Te and Nb are mainly attributed to the difference between their chemical components. The results of our work agree well with the previous calculations [10, 20] (Table 2).

TABLE 2. Adsorption energies (eV) of Te at different sites on the Ni(111) and Nb-Ni(111) surfaces. (See Fig. 1 for the atomic sites.)

Atoms	ΔE (eV)	Chemical component (eV)	Mechanical component (eV)
Te (this work)	2.16	0.14	2.01
Te (Ref. [10])	1.6	−0.2	1.8
Nb (this work)	−1.03	−2.89	1.86
Nb (Ref. [20])	−1.05	–	–

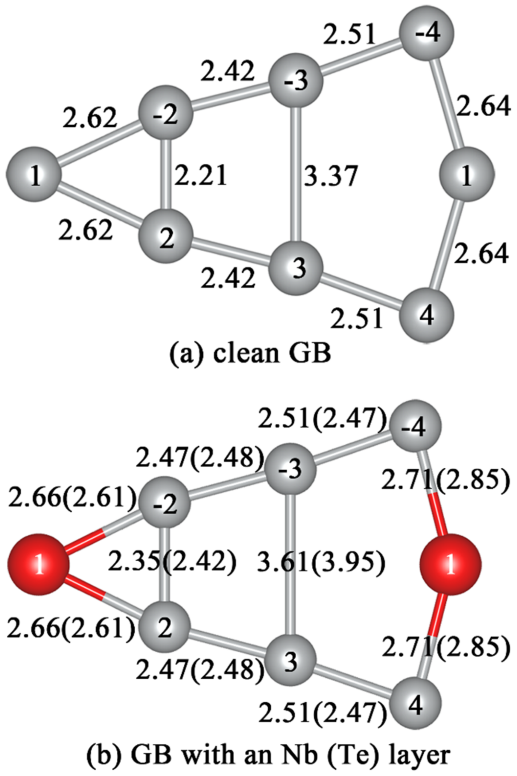

Fig. 3. (Color online) Calculated interatomic distances (Å) in the GB region for (a) clean GB, and (b) GB + 4 Nb in Layer 1 (a Nb layer) and the GB + 4 Te in Layer 1 (a Te layer). The data for the case of Te are given in parenthesis. The atoms are marked by their site numbers.

D. Chemical bonds and electronic structures

The atomic and electronic structures were studied for mechanisms of the different effects of Te and Nb on Ni GB. The calculated interatomic distances in the GB region are shown in Fig. 3 for the comparison. Being bigger than Ni in atomic radius, Te and Nb induce the GB expansion, as shown in Fig. 3. For example, comparing with in the clean GB, the Ni(3)-Ni(-3) distances in the GBs + Te layer and

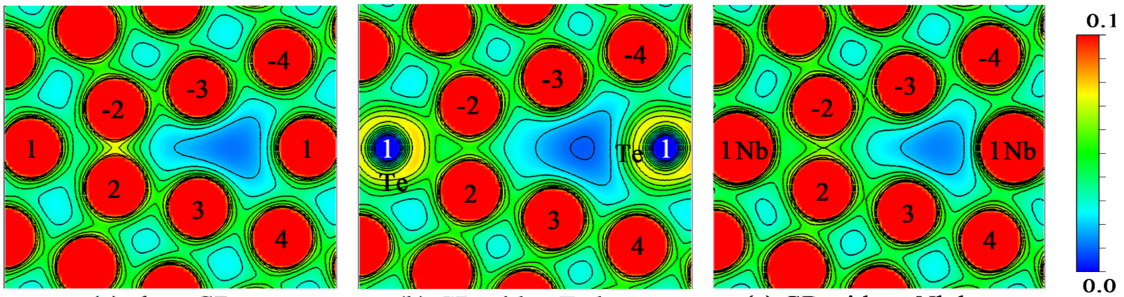

Fig. 4. (Color online) Calculated charge density distribution (electron/Bohr^3) in the (100) plane for (a) clean GB, (b) GB + Te layer and (c) GB + Nb layer. The atoms of interest are marked by their site numbers.

GBs + Nb layer are elongated by 0.58 Å and 0.24 Å, respectively. The expansion can impair the GB cohesion, which is in accordance with the positive values of the strengthening/embrittling energies for Te and Nb. Also, it can be seen in Fig. 3 that the Te-induced GB expansion is more serious than the Nb-induced expansion, as the larger positive mechanical component of Te is bigger than Nb.

The chemical component of the strengthening/embrittling energy is thought to be induced by the charge redistribution due to the existence of the doped atoms [10]. With only a small difference in mechanical components for Te and Nb (see Table 2), their chemical components are comparable. Fig. 4 shows the calculated charge density distributions for the clean GB, GB + Te layer and GB + Nb layer. The Te(1)-Ni(2)/Ni(-2) bond in Fig. 4(b) and Nb(1)-Ni(2)/Ni(-2) bond in Fig. 4(c) are stronger than the corresponding Ni(1)-Ni(2)/Ni(-2) bond in Fig. 4(a), as judged by the charge densities along these bonds. But these strong Te-Ni bonds cannot enhance the GB cohesion that much, since directions of the bonds are almost in parallel with the GB plane. On the other hand, the Ni(2)-Ni(-2) and Ni(1)-Ni(4)/Ni(-4) bonds are normal to the GB plane and exert the main cohesive force to hold the two grains together as displayed in Fig. 4(a). Replacing Ni with Te in Fig. 4(b) makes the Ni(2)-Ni(-2) bond much weaker than the corresponding Ni(2)-Ni(-2) bond in Fig. 4(a). However, for the GB with a Nb layer in Fig. 4(c), the Ni(2)-Ni(-2) bond is a little weaker than the corresponding Ni(2)-Ni(-2) bond in Fig. 4(a), but the Nb(1)-Ni(4)/Ni(-4) bond is obviously stronger than the Ni(1)-Ni(4)/Ni(-4) bond in Fig. 4(a). As a result, the remarkable differences between the chemical components of the strengthening/embrittling energies for Te and Nb are induced by these charge redistributions. The charge density for the GB + Te layer in Fig. 4(b) is in accordance with the result in Ref. [10].

As the conjugation interface between two misoriented grains, GB severs an ideal channel for migration of corrosive elements (e.g. Te in our case) to induce the SCC. As an additive to the alloy, Nb can segregate to the GB and enhance the GB cohesion, which can reduce the intergranular Te cracking. The strong Nb-Ni bonds in the GB region can also prevent the migration of Te along the GB to the inside of the alloy. In the meanwhile, MSRE found that Nb can also improve the resistance of Ni-based Hastelloy N to irradiation embrittlement, but this effect of Nb is likely not useful at operating temperatures much above 650 °C [4, 5]. Our work sheds lights on the effect of Nb additive on the Te-induced SCC in Hastelloy N on the atomic and electronic level, and is very helpful to the design of modified Hastelloy N with new additive that can further improve the resistances to intergranular embrittlement by Te and irradiation embrittlement at elevated temperature simultaneously.

IV. CONCLUSION

First-principles calculations were performed to research the effect of Nb additive on the Te-induced GB embrittlement in Ni alloy. Energetic studies have shown that Te atoms don't tend to form the surface-reaction layer with Nb on the surface of Ni alloy. And Nb atoms on the surface cannot prevent the preferred diffusion of Te atoms along the GBs. On the other hand, the first-principles tensile tests have shown that the Nb segregation in GB can inhibit the Te-induced GB embrittlement. The strong Nb-Ni bonds in the GB region can improve the GB cohesion and prevent the migration of Te along the GBs. The strengthening/embrittling energies of Nb and Te were calculated. The chemical bonds and electronic structures were analyzed to uncover the physical origin of the mechanical and chemical components of the strengthening/embrittling energies.

[1] Generation IV International Forum. A Technology Roadmap for Generation IV Nuclear Energy Systems. U.S. DOE, GIF-002-00, Dec. 2002.

[2] Rosenthal M W, Briggs R B, Haubenreich P N. Molten-salt reactor program, semiannual progress report, ORNL-4782. Oak Ridge, Tennessee, USA, 1972.

[3] Rosenthal M W, Haubenreich P N, Briggs R B. The development status of molten-salt breeder reactors, ORNL-4812. Oak Ridge, Tennessee, USA, 1972.
[4] Keiser J R. Status of tellurium-Hastelloy N studies in molten fluoride salts, ORNL/TM-6002. Oak Ridge, Tennessee, USA, 1977.
[5] McCoy H E Jr. Status of materials development for molten salt reactors, ORNL/TM-5920. Oak Ridge, Tennessee, USA, 1978.
[6] Wu R Q, Freeman A J, Olson G B. Science, 1994, **265**: 376–380.
[7] Yamaguchi M, Shiga M, Kaburaki H. Science. 2005, **307**: 393–397.
[8] Yuasa M and Mabuchi M. Phys Rev B, 2010, **82**: 094108.
[9] Liu W G, Han H, Ren C L, *et al*. Comp Mater Sci, 2014, **88**: 22–27.
[10] Vsianska M and Sob M. Prog Mater Sci, 2011, **56**: 817–840.
[11] Hohenberg P, ohn W. Phys Rev B, 1964, **136**: 864–871.
[12] Kohn W and Sham L J. Phys Rev, 1965, **140**: A1133–A1138.
[13] Kresse G and Furthmuller J. Phys Rev B, 1996, **54**: 11169–11186.
[14] Blochl P E. Phys Rev B, 1994, **50**: 17953–17979.
[15] Perdew J P, Chevary J A, Vosko S H, *et al*. Phys Rev B, 1992, **46**: 6671–6687.
[16] Rice J R and Wang J S. Mat Sci Eng A-Struct, 1989, **107**: 23–40.
[17] Geng W T, Freeman A J, Wu R, *et al*. Phys Rev B, 1999, **60**: 7149–7155.
[18] Lozovoi A Y, Paxton A T, Finnis M W. Phys Rev B, 2006, **74**: 155416.
[19] Wachowicz E, Ossowshi T, Kiejna A. Phys Rev B, 2010, **81**: 094104.
[20] Geng W T, Freeman A J, Olson G B. Phys Rev B, 2001, **63**: 165415.